

Involvement of the dentate nucleus in the pathophysiology of amyotrophic lateral sclerosis: A multi-center and multi-modal neuroimaging study



Komal Bharti^a, Muhammad Khan^a, Christian Beaulieu^b, Simon J. Graham^c, Hannah Briemberg^d, Richard Frayne^e, Angela Genge^f, Lawrence Korngut^g, Lorne Zinman^c, Sanjay Kalra^{a,b,*}, for the Canadian ALS Neuroimaging Consortium

^a Department of Medicine, Division of Neurology, University of Alberta, Edmonton, Alberta, AB, Canada

^b Department of Biomedical Engineering, University of Alberta, Edmonton, Alberta, AB, Canada

^c Sunnybrook Health Sciences Centre, University of Toronto, Toronto, Ontario, Canada

^d Department of Medicine, Division of Neurology, University of British Columbia, Vancouver, BC, Canada

^e Departments of Radiology and Clinical Neurosciences, Hotchkiss Brain Institute, University of Calgary, and Seaman Family MR Research Centre, Foothills Medical Centre, Calgary, Alberta, AB, Canada

^f Montreal Neurological Institute and Hospital, McGill University, Montreal, Quebec, Canada

^g Department of Clinical Neurosciences, Hotchkiss Brain Institute, University of Calgary, Foothills Medical Centre, Calgary, Alberta, AB, Canada

ARTICLE INFO

Keywords:

Amyotrophic lateral sclerosis
Dentate nucleus
Resting-state functional magnetic resonance imaging
Resting-state functional connectivity
Diffusion tensor imaging

ABSTRACT

Amyotrophic lateral sclerosis (ALS) is characterized primarily by motor neuron but also frontotemporal lobar degeneration. Although the cerebellum is involved in both motor and cognitive functions, little is known of its role in ALS. We targeted the dentate nucleus (DN) in the cerebellum and the associated white matter fibers tracts connecting the DN to the rest of the brain using multimodal imaging techniques to examine the cerebellar structural and functional connectivity patterns in ALS patients and hypothesized that the DN is implicated in the pathophysiology of ALS. A cohort of 127 participants (56 healthy subjects (HS); 71 ALS patients) were recruited across Canada through the Canadian ALS Neuroimaging Consortium (CALSNIC). Resting state functional MRI, diffusion tensor imaging (DTI), and 3D weighted T1 structural images were acquired on a 3-tesla scanner. The DN in the cerebellum was used as a seed to evaluate the whole brain cerebral resting-state functional connectivity (rsFC). The superior cerebellar peduncle (SCP), middle cerebellar peduncle (MCP) and inferior cerebellar peduncle (ICP) were used as a region of interest in DTI to evaluate the structural integrity of the DN with the cortex and brain stem. Cerebellar volumetric analysis was done to examine the lobular and DN grey matter (GM) changes in ALS patients. Lastly, an association between DN rsFC and structural alterations were explored. DN rsFC was reduced with cerebrum (supplementary motor area, precentral gyrus, frontal, posterior parietal, temporal), lobule IV, and brain stem, and increased with parieto-occipital region. DN rsFC and white matter (WM) diffusivity alterations at SCP, MCP, and ICP were accompanied by correlations with ALSFRS-R. There were no DN volumetric changes. Notably, DN rsFC correlated with WM abnormalities at superior cerebellar peduncle. The DN plays a pathophysiological role in ALS. Impaired rsFC is likely due to the observed cerebellar peduncular WM damage given the lack of GM atrophy of the DN. This study demonstrates altered cerebellar rsFC connectivity with motor and extra-motor regions in ALS, and impaired rsFC is likely due to the observed cerebellar peduncular WM damage given the lack of GM atrophy of the DN. The correlation between the altered DN connectivity, and the behavioral data support the hypothesis that the DN plays a pathophysiological role in ALS.

1. Introduction

Amyotrophic lateral sclerosis (ALS) is a motor neuron disorder which leads to progressive neurodegeneration and an ultimate death

within a few years of disease onset (Rowland and Shneider, 2001; del Aguila et al., 2003; Beghi et al., 2006; Alonso et al., 2009; Hardiman et al., 2011). ALS is characterized by an increase in the upper motor neuron (UMN) burden in the motor cortex and lower motor neuron

* Corresponding author: Department of Medicine (Neurology), Neurosciences and Mental Health Institute, University of Alberta, 7-132F Clinical Sciences Building, 11350-83 Ave Edmonton, Alberta T6G 2G3, Canada.

E-mail address: kalra@ualberta.ca (S. Kalra).

burden in the brain stem and spinal cord, leading to the fatal failure of motor functions (Rowland and Shneider, 2001; Turner, 2011). However, in the past few decades, researchers have determined that ALS affects both motor and extra-motor brain areas such as those responsible for maintaining cognition, executive functions and behavior (Phukan et al., 2007, 2012; Easterling et al., 2013; Goldstein and Abrahams, 2013; Abrahams et al., 2014). Despite the recent progress in ALS research, the pathophysiology underpinning the ALS disease is believed to be very complex and requires much further investigation.

Magnetic resonance imaging (MRI) studies have yielded valuable insights about the pathophysiology of ALS. One such MRI technique is resting state functional magnetic resonance imaging (rs-fMRI); an imaging modality that captures low frequency fluctuations in blood oxygen level-dependent (BOLD) signals in the absence of an overt behavioral task (Biswal et al., 1995; Biswal, 2012). The technique detects disturbances in resting state networks (RSNs) corresponding to functional abnormalities in widespread cortical and subcortical brain regions (Smith et al., 2009). Previous rs-fMRI studies in ALS have primarily reported the involvement of both motor and extra-motor brain regions i.e. the precentral gyrus, supplementary motor area, frontal, temporal, parieto-occipital areas and the cerebellum (Mohammadi et al., 2009; Jelsone-Swain et al., 2010; Verstraete et al., 2010; Agosta et al., 2011, 2013; Douaud et al., 2011; Luo et al., 2012; Tedeschi et al., 2012; Zhou et al., 2013, 2016; Heimrath et al., 2014; Chenji et al., 2016; Menke et al., 2016; Qiu et al., 2019). Additionally, structural MRI studies have reported grey matter (GM) alterations in cortical brain areas i.e. the precentral gyrus, parietal and occipital areas along with the subcortical areas such as the cerebellum (Kassubek et al., 2005; Agosta et al., 2007, 2012; Thivard et al., 2007; Verstraete et al., 2010; Douaud et al., 2011; Ferraro et al., 2017; Menke et al., 2017; Shen et al., 2018). Diffusion tensor imaging (DTI) studies have also reported altered diffusivity in the cerebellum, insula, corpus callosum, corticospinal tract and the frontal, temporal and occipital areas (Agosta et al., 2007; Thivard et al., 2007; Verstraete et al., 2010; Canu et al., 2011; Douaud et al., 2011; Bede et al., 2015; Trojsi et al., 2015; Femiano et al., 2018). Altogether, these findings across multiple different MRI measures suggest a consistent feature of structural and functional impairment of the cerebellum in ALS.

The cerebellum is considered a crucial subcortical brain structure responsible for not only controlling movement, but also for maintaining higher-level cognitive functions (Schmahmann and Sherman, 1998; Middleton and Strick, 2000; Strick et al., 2009; Buckner, 2013; Kozlak et al., 2014; Moberget and Ivry, 2019). The involvement of the cerebellum has been frequently studied in other neurodegenerative disorders (Fasano et al., 2017; Mormina et al., 2017; Tona et al., 2017; Bharti et al., 2019; Qiu et al., 2019); however, no neuroimaging study in ALS has so far investigated, as its primary focus, the cerebellum and its connection with the rest of the brain. Thus, to address this gap in knowledge, we specifically targeted the deep brain cerebellar nuclei and in particular the dentate nucleus (DN) to investigate the structural and functional MRI alterations in the cortical and subcortical brain structures of the cerebral cortex.

The DN acts as a connecting channel for the flow of input and output signals between the cerebellum and the motor and extra-motor brain areas of cerebral cortex (Dum et al., 2002; Dum and Strick, 2003; Diedrichsen et al., 2011; Akakin et al., 2014; Bernard et al., 2014). The DN coordinates motor functions by projecting signals to the primary motor and premotor areas of the cerebral cortex; thereby regulating balance, posture, and voluntary movements (Chan-Palay et al., 1977; Brazis et al., 1981; Asanuma et al., 1983; Hoover and Strick, 1999). The DN also coordinates extra-motor functions, such as cognitive behavior, by relaying signals to the prefrontal and posterior parietal brain areas of the cerebral cortex (Middleton and Strick, 1996, 2001; Kelly and Strick, 2003; Salamon et al., 2007; Suzuki et al., 2012).

We hypothesized that the cerebellar DN is implicated in the pathophysiology of ALS. Neuropathological studies have already

underlined the role of the DN in the degeneration of ALS patients (Nakano et al., 2004; Geser et al., 2008; Mochizuki et al., 2012). Therefore, to better understand the role of the DN in the pathophysiology of ALS, we investigated the structural and functional cerebral alterations with respect to the cerebellar DN in a multicenter study using three complementary neuroimaging techniques: rs-fMRI, DTI and voxel-based morphometry (VBM). With rs-fMRI, we explored seed-to-voxel whole-brain rsFC using the cerebellar DN as a seed. With DTI, we examined microstructural WM diffusivity along the superior, middle and inferior cerebellar peduncles. VBM analysis was used to examine the GM volumes of the cerebellar lobules and DN. In ALS patients, clinical correlations were sought with the structural and functional measures. Lastly, the association between DN rsFC and structural changes was explored.

2. Materials and methods

2.1. Canadian ALS neuroimaging consortium

In the current study, the neuroimaging and clinical data acquisition was done across Canada through the Canadian ALS Neuroimaging Consortium (CALSNIC) using a standardized protocol. The 5 sites of data acquisition were: University of Alberta, Edmonton; University of British Columbia, Vancouver; University of Calgary, Calgary; McGill University, Montreal; and University of Toronto, Toronto.

2.2. Participants

The study includes a total cohort of 127 subjects (56 healthy subjects (HS); 71 ALS). All the patients were diagnosed as possible, probable, or definite ALS according El Escorial Criteria (Brooks, 1994). The exclusion criteria included patients with other neurological and psychiatric illness, especially primary lateral sclerosis, progressive muscular atrophy, fronto-temporal dementia, and cerebellar ataxia. The study was conducted in acceptance with the approval of the research ethics boards across all the CALSNIC sites. First, written informed consents forms were obtained from all the participants and then were instructed to lie down straight in a fully awake and relaxed condition. Demographic and clinical details of ALS patients and HS are summarized in Table 1.

2.3. Clinical assessment

Estimated scores of UMN burden were derived for the patients from their clinical assessments. ALS disease severity was measured using the ALS functional rating scale - Revised (ALSFRS-R) (Cedarbaum et al., 1999), an instrument which quantifies disease based on 12 different measures such as speech, salivation, swallowing, handwriting, walking, climbing stairs, and breathing. The range of ALSFRS-R scores varies from 0 to maximum of 48. Decreased scores of ALSFRS-R represent higher clinical disability indicating functional impairment. Based on the ALSFRS-R scores, a disease progression rate was calculated as 48-ALSFRS-R/symptom duration (Kimura et al., 2006). Severity of motor neuron dysfunction was assessed individually for each participant by calculating the UMN burden scores. Examination of motor symptoms included finger tapping and foot tapping tasks for each side, respectively. For finger tapping, participants were instructed to tap the index finger as fast as possible within the time frame of 10 s. For foot tapping, participants were asked to tap their foot under the same instructions. The number of taps were recorded and averaged for each side. Examination of extra-motor symptoms included testing of cognitive functions using the Edinburgh Cognitive and Behavioral ALS screen (ECAS) test (Niven et al., 2015). Neurological examinations, such as assessment of muscle stretch reflexes, were performed by a neurologist at each CALSNIC site.

Table 1

Demographic and clinical features of ALS patients and healthy subjects.

Variables	ALS patients (n = 71)	Healthy subjects (n = 56)	p value
Age(yrs)	59.3 ± 11.2	55.2 ± 9.7	0.002*
Male/Female	78/52	60/59	0.12
ALSFRS-R	37.5 ± 6.42	–	–
Symptom Duration (months)	33.2 ± 26.2	–	–
Disease Duration (months)	0.49 ± 0.51	–	–
ECAS-Total	106.26 ± 15.30	112.28 ± 12.43	0.0004*
ECAS specific	78.71 ± 13.16	83.58 ± 10.00	0.0006*
ECAS non-specific	27.54 ± 3.75	28.69 ± 3.78	0.01*
Right Finger Tapping (10 s)	36.8 ± 20.8	55.5 ± 20.9	0.00001*
Left Finger Tapping (10 s)	33.5 ± 18.6	49.6 ± 19.02	0.00001*
Right Foot Tapping (10 s)	23.4 ± 16.0	39.6 ± 14.3	0.00001*
Left Foot Tapping (10 s)	21.6 ± 15.5	59.6 ± 31.4	0.00001*
UMN Burden	5.0 ± 3.5	–	–

ALS: Amyotrophic Lateral Sclerosis; ALSFRS-R: Amyotrophic Lateral Sclerosis Functional Rating Scale - Revised; ECAS: Edinburgh Cognitive and Behavioural ALS Screen; UMN: Upper Motor Neuron. Values are reported as mean ± SD.

Values are reported as mean ± SD.

Differences in the demographic and clinical scores between ALS patients and healthy subjects were assessed by unpaired t test.

Differences in the gender between ALS patients and healthy subjects were assessed by χ^2 test.

2.4. Imaging protocol

The structural and functional imaging was performed at each CALSNIC site using MRI systems operating at 3 T. The imaging protocol used was standardized across all centres (Table 2).

2.5. Data analysis

2.5.1. Resting-state fMRI (rs-fMRI) data analysis

The rs-fMRI data analysis was performed using FSL (FMRIB software library package) (<http://www.fmrib.ox.ac.uk/fsl>) (Smith et al., 2004). The single subject pre-processing of rs-fMRI data and higher level

processing was performed by fMRI Expert Analysis Tool (FEAT, <http://www.fmrib.ox.ac.uk/fslwiki>) (Jenkinson et al., 2012). The pre-processing steps included brain extraction of 3D-weighted T1 images using the brain extraction tool (BET), head motion correction using the MCFLIRT tool, slice timing correction, and spatial smoothing using a Gaussian kernel with a full width at half maximum of 5 mm and a high pass temporal filtering cutoff of 100 s. Higher level processing included the linear registration of functional images with the processed BET images using the FMRIB linear image registration tool (<http://www.fmrib.ox.ac.uk/fsl/FLIRT>). The output of linear registration was then non-linearly registered with the Montreal Neurological Institute (MNI) standard space using the FMRIB nonlinear image registration tool (<http://www>.

Table 2

Details of MRI data acquisition across different sites.

CALSNIC Site	University of Alberta	University of British Columbia	University of Calgary	McGill University	University of Toronto
Scanner model	Siemens 3 Tesla Prisma	Philips 3 Tesla Intera	GE 3 Tesla Discovery MR 750	Siemens 3 Tesla Triotrim	GE 3 Tesla Discovery MR 750
Software version	syngo MR E11	3.2.31	DV25.0_EB_1442.a	syngo MR B17	DV25.0_EB_1442.a
3D T₁-weighted scan, axial acquisition					
Repetition time, ms	2300	7.9	min (7.4)	2300	min (7.4)
Echo time, ms	3.43	3.5	min (3.1)	3.43	min (3.1)
Inversion time, ms	900	950	400	900	400
Flip angle, degrees	9	8	11	9	11
Field of view, mm	256 × 256	240 × 240	256 × 256	256 × 256	256 × 256
Matrix dimension, pixels	256 × 256	240 × 240	256 × 256	256 × 256	256 × 256
Voxel dimension, mm	1 × 1 × 1	1 × 1 × 1	1 × 1 × 1	1 × 1 × 1	1 × 1 × 1
Slices, n	176	150	176	176	176
Acquisition times, min	05:30	06:08	04:30	05:30	04:30
Diffusion Tensor Imaging, axial acquisition					
Repetition time, ms	10,000	11,848	9000	10,000	9000
Echo time, ms	90.0	56.0	min (80)	90.0	min (80)
Field of view, mm	256 × 256	256 × 256	256 × 256	256 × 256	256 × 256
Matrix dimension, pixels	128 × 128	128 × 128	128 × 128	128 × 128	128 × 128
Voxel dimension, mm	2 × 2 × 2	2 × 2 × 2 ⁴	2 × 2 × 2	2 × 2 × 2	2 × 2 × 2
Diffusion directions, n	30	30	30	30	30
Diffusion b-value	1000	1000	1000	1000	1000
Diffusion images with b = 0	5	5	5	5	5
Slices, n	70	70	70	70	70
Acquisition times, min	07:40	06:31	05:24	07:40	05:24
Resting-state functional MRI, axial acquisition					
Repetition time, ms	2200	2200	2200	2200	2200
Echo time, ms	30.0	30.0	30.0	30.0	30.0
Flip angle, degrees	70	70	70	70	70
Field of view, mm	224 × 224	224 × 224	224 × 224	224 × 224	224 × 224
Matrix dimension, pixels	64 × 64	64 × 64	64 × 64	64 × 64	64 × 64
Voxel dimension, mm	3.5 × 3.5 × 3.5	3.5 × 3.5 × 3.5	3.5 × 3.5 × 3.5	3.5 × 3.5 × 3.5	3.5 × 3.5 × 3.5
Trains, n	192	192	192	192	192
Slices, n	40	40	40	40	40
Acquisition times, min	07:00	07:16	07:00	07:00	07:00

fmrib.ox.ac.uk/fsl/fslwiki/FNIRT.

2.5.1.1. Motion parameter analysis. The results of rsFC analyses may be affected by head motion (Maknojia et al., 2019). To query for the potential effect of head motion in the current analysis, we first calculated the mean absolute and relative head motion displacement values using the MCFLIRT tool in FSL. The mean and relative head motion displacement values of ALS patients and HS were then assessed for statistical differences using the two-sample unpaired *t*-test through SPSS (SPSS Inc., Chicago, IL, USA).

2.5.1.2. Seed description (dentate nucleus). The mask of the DN was obtained from a high resolution 3D-T1 image using the FMRIB's Integrated Registration and Segmentation tool (<http://fsl.fmrib.ox.ac.uk/fsl/fslwiki/FIRST>), an automatic subcortical segmentation program. Based on previous literature, a spherical region of interest (ROI) of 2 mm radius was created for the DN seed using the coordinates (left $x = -17$, $y = -58$, $z = -35$; right $x = 17$, $y = -56$, $z = -35$) on the standard MNI_2-mm template in the FSL toolbox (Diedrichsen et al., 2011). A single bilateral mask was obtained by merging the left and right mask of the DN which was then transformed from the MNI_2-mm template space to the individual participant functional data space, using the combined linear and non-linear deformation matrix. After the successful transformation, we carefully visualized every subject data in a functional space to ensure an appropriate overlap between the DN seed in standard space and individual functional data space. The related average rs-fMRI time course for the DN seed was then extracted and inserted into FEAT to produce the individual participant-level correlation maps for all the voxels (family-wise error [FWE], corrected at $p < 0.05$). The positive and negative DN functional correlation maps were obtained individually for every participant and then were used to perform group level comparisons using FEAT. The statistical differences between the ALS patients and HS were assessed using the two-sample unpaired *t* test in a multiple linear regression model implemented in FSL. The DN seed-to-voxel whole brain rsFC results were first transformed into Z statistic images and then later thresholded at a cluster level of $Z > 2.3$, corrected for multiple comparisons according to a whole brain family-wise error (FWE) of $p < 0.05$. Lastly, the anatomical localization of significant clusters was obtained using the Harvard-Oxford Cortical and Subcortical Structural Atlas and Probabilistic Cerebellar Atlas, included in FSL.

2.5.1.3. Nuisance signal regression analysis and covariates of no interest. To remove the effect of noise, we first obtained rs-fMRI time courses for cerebrospinal fluid (CSF) and WM for every participant. Masks corresponding to CSF and WM regions for every participant were transformed to functional data space, using the combined linear and non-linear deformation matrix to extract the related average time course series (Gavrilescu et al., 2002; Macey et al., 2004). The average time courses for CSF and WM were added as covariates of no interest into the multiple linear regression model of FSL. Furthermore, age, sex, motion parameters, effect of MRI scanner, and site of data acquisition were also added.

2.5.1.4. Clinical correlations. A correlation analysis was performed between the DN rsFC differences and the clinical scores i.e. ALSFRS-R, disease progression rate, symptom duration, finger and foot tapping scores (right and left side; separately), UMN burden and ECAS scores. Statistical differences were assessed using the multiple linear regression model in FSL, a threshold-free cluster enhancement technique (TFCE) and a non-parametric test of 5000 random permutation with covariates of no interest i.e. age, gender, motion parameters, effect of MRI scanner, and site of data acquisition. The DN rsFC clinical correlation results were corrected for multiple comparisons with the FWE set at $p < 0.05$.

2.5.2. Diffusion tensor imaging (DTI) analysis

The data analysis was performed using FSL (FMRIB software library package) (<http://www.fmrib.ox.ac.uk/fsl>) (Smith et al., 2004). Pre-processing included the extraction of non-brain voxels using BET in FSL, as well as motion correction and eddy current correction. The resultant output data were then subjected to DTI Fit using FMRIB's diffusion toolbox (<http://fsl.fmrib.ox.ac.uk>) to generate fractional anisotropy (FA) maps along with mean diffusivity (MD), axial diffusivity (AD) and radial diffusivity (RD) maps.

The FA maps were then processed for voxel-wise statistical analysis using the Tract-Based Spatial Statistical (TBSS) tool (<https://fsl.fmrib.ox.ac.uk/fsl/fslwiki>) (Smith et al., 2006). Individual FA maps were aligned in a common space by using non-linear image registration tool. We opted to use the FMRIB58_FA_1-mm image as the target for non-linear image registration, the most recommended option suggested in TBSS online instructions. The individual FA maps for each participant were first non-linearly registered with the target image i.e. FMRIB58_FA template and then were linearly transformed into the MNI standard space at 1 mm isotropic resolution, where they were averaged to create the mean FA image. The mean FA image was subsequently thinned to create the mean FA skeleton at a threshold of 0.2, which represented the common center of the WM tracts. The resultant FA maps were then fed into multiple linear regression model for the voxel-wise cross participant statistics to compute the group differences between ALS patients and HS using the two-sample unpaired *t* test with covariates of no interest i.e. age, gender, motion parameters, effect of MRI scanner, and site of data acquisition. The statistical analysis was computed by using the TFCE technique including non-parametric testing with 5000 random permutations (Smith and Nichols, 2009). The final results were reported after correcting for multiple comparisons at the FWE of $p < 0.05$. The JHU ICBM-DTI-81 white matter atlas in the FSL library was then used to prepare regions of interest for the superior cerebellar peduncle (SCP), middle cerebellar peduncle (MCP), and inferior cerebellar peduncle (ICP). The MD, AD and RD maps were processed using the same approach.

2.5.2.1. Clinical correlations. A correlation analysis was performed between the DTI findings at the three cerebellar peduncles and the clinical scores i.e. ALSFRS-R, disease progression rate, symptom duration, finger and foot tapping scores (right and left side; separately), UMN burden and ECAS scores. Statistical differences were assessed using the multiple linear regression model in FSL and TFCE technique with non-parametric testing involving 5000 random permutations and covariates of no interest i.e. age, gender, motion parameters, effect of MRI scanner, and site of data acquisition. The DTI clinical correlation results were corrected for multiple comparisons at the false discovery rate (FDR) of $p < 0.05$.

2.5.3. Cerebellar volumetric analysis

The cerebellar volumetric analysis of ALS patients and HS was performed on the 3D-weighted T1 images using the Spatially Unbiased Infratentorial toolbox (SUIT) (<http://www.diedrichsenlab.org/imaging.suit.htm>) implemented in SPM 12 (<http://www.fil.ion.ucl.ac.uk/spm>). The SUIT toolbox provides a high resolution atlas template for the cerebellum which is unbiased and preserves the anatomical details of the cerebellar lobules (Diedrichsen, 2006). For this purpose, first the individual 3D-weighted T1 images were subjected to automatic isolation and segmentation to extract the cerebellum and its corresponding cerebellar mask in the participant-specific native space. The non-brain voxels in the cerebellar mask were carefully inspected and wherever necessary subjected to manual adjustments. Secondly, the extracted cerebellum was normalized using an option "dentate nucleus as a ROI" to provide a good overlap between the isolated cerebellum and the SUIT atlas template space. This step transformed the isolated cerebellum from native participant space to the SUIT atlas template space i.e. the cerebellum template using the affine transformation matrix and

non-linear flow field. In the third step, the cerebellum data for each participant was resliced to modulate and preserve the amount of different cerebellar lobular volumes in the SUIT atlas template space. Lobular volumes were subsequently calculated by using the sum of the hemispheres and vermis. The global volume of the cerebellum, along with the anterior and posterior volume of the cerebellum, were calculated as the sum of lobules I-IV and VI-X. Statistical differences in the cerebellar lobular volumes of ALS patients and HS were assessed by using the two-sample *t* test in SPSS software (SPSS Inc., Chicago, IL, USA).

2.5.3.1. DN cerebellar volumetric analysis. To investigate the GM cerebellar volumetric differences within the mask of the DN seed, the normalized MR images in the SUIT atlas template space were subjected to small volume correction in order to concisely restrict the findings to ROI. Using SPM, a two-sample *t* test was performed to assess the possible differences between ALS patients and HS (corrected for multiple comparisons at FWE of $p < 0.05$).

2.5.4. Correlation analysis between the DN rsFC and DTI

In ALS, a correlation analysis was performed between the z scores of DN rsFC and the z scores of altered white matter diffusivity at the three cerebellar peduncles. Significant differences were assessed using spearman's rank correlation in SPSS (SPSS, Chicago, IL, USA).

3. Results

Table 1 summarizes the demographic and clinical characteristics of the sample populations. No significant differences in age and gender were observed between ALS patients and HS (all $p > 0.05$). The mean ECAS scores, and respective finger and foot tapping scores of each side were significantly lower in ALS patients than HS.

3.1. Resting-state fMRI (rs-fMRI) results

3.1.1. Motion parameters

The mean absolute head displacement values were 0.287 ± 0.211 mm in ALS patients and 0.259 ± 0.144 mm in HS. The mean relative head displacement values were 0.096 ± 0.09 mm in ALS patients and 0.085 ± 0.03 mm in HS. Neither metric showed significant group differences: the p value of the mean absolute head displacement between ALS patients and HS was 0.42; and the p value of the mean relative head displacement between ALS patients and HS was 0.44.

3.1.2. Group differences

Compared to HS, ALS patients exhibited lower rsFC between the DN and motor regions, namely the right precentral gyrus and bilateral supplementary motor area (SMA). The rsFC was also decreased between DN and lobule IV of the left cerebellum and the brain stem. In addition, ALS patients had lower rsFC between DN and extra-motor brain regions, including bilateral anterior cingulate cortex, right frontal pole, inferior and middle frontal gyri, frontal and central operculum cortex, frontal orbital cortex, temporal pole, supramarginal, angular, and postcentral gyri. In contrast, ALS patients also displayed higher rsFC between the DN and parieto-occipital brain regions i.e. lateral occipital cortex, temporal occipital fusiform cortex, occipital fusiform gyrus, occipital pole, lingual gyrus, and supracalcarine cortex bilaterally (**Fig. 1**; **Table 3**).

3.1.3. Clinical correlations

In ALS patients, rsFC between DN and lobule IV of the left cerebellum along with the brain stem positively correlated with ALSFRS-R. Similarly, rsFC between DN and right inferior frontal gyrus, anterior cingulate cortex and precentral gyrus positively correlated with the ECAS and left foot tapping scores. The reported results were corrected

for multiple comparisons at FWE approach at $p < 0.05$ (**Fig. 2**).

3.2. DTI results

3.2.1. Group differences

As compared to HS, ALS patients exhibited lower FA at the SCP and ICP. ALS patients also exhibited higher AD and RD at the SCP and MCP. The reported results are corrected for multiple comparisons at FWE $p < 0.05$ (**Fig. 3**). No significant differences were observed in MD at SCP, MCP, and ICP.

3.2.2. Clinical correlations

In ALS patients, FA at SCP and ICP negatively correlated with the disease progression rate and UMN burden scores and positively correlated with ALSFRS-R, right finger tapping, right foot tapping and left foot tapping scores. The AD and RD at SCP and MCP positively correlated with disease progression rate and UMN burden scores and negatively correlated with ALSFRS-R, right finger tapping, right foot tapping and left foot tapping scores. The reported results were corrected for multiple comparisons at FDR approach of $p < 0.05$. **Fig. 4** shows the clinical correlations of FA, AD and RD at SCP. Clinical correlations for AD, RD at MCP and FA at ICP were identical as SCP and thus are not displayed. The results were corrected for multiple comparisons at FDR approach of $p < 0.05$.

3.3. Cerebellar volumetric results

The average global cerebellar GM volume was 111.90 ± 24.8 mL in ALS patients and 112.71 ± 29.8 mL in HS. No significant differences in the global, lobular, or cerebellar DN GM volume were observed between ALS patients and HS (all $p > 0.05$).

3.4. Correlations between the DN rsFC and DTI findings

In ALS patients, a positive correlation was present between lower DN rsFC and lower FA at SCP (**Fig. 5a**). Similarly, higher DN rsFC showed negative correlation with lower FA at SCP (**Fig. 5b**). The reported results were first corrected for $p < 0.05$ using Spearman's rank correlation in SPSS and then later the graphs were plotted using MATLAB in SPM12.

4. Discussion

The objective of this study was to investigate cerebellar pathology with a focus on the DN in ALS using multimodal MRI in a multicenter study. For this, we examined the rsFC between the DN in the cerebellum and the whole brain cerebral cortex, microstructural WM integrity at the three cerebellar peduncles, and the GM volume of the cerebellar lobules and DN. When compared with HS, ALS patients exhibited altered cerebellar DN rsFC in several cortical and subcortical brain regions of the cerebral cortex which further correlated with clinical measures such as ALSFRS-R, ECAS, and tapping scores. Substantial DTI abnormalities were also present in the white matter fiber tracts of the SCP, MCP, and ICP with significant clinical correlations. To our surprise, we observed no DN cerebellar volumetric differences in ALS patients as compared to HS. Last, in ALS patients the DN rsFC significantly correlated with the altered DTI metrics. The findings suggest that altered functional connectivity between the cerebellum and cerebral cortical and subcortical areas is likely a result of WM degeneration of the cerebellar peduncles connecting these regions.

4.1. rsFC between the DN and the motor brain regions

The rsFC between the DN and the motor brain regions (i.e. SMA and precentral gyrus) was lower in ALS patients than in HS. ALS studies have reported functional alterations in the SMA and precentral gyrus

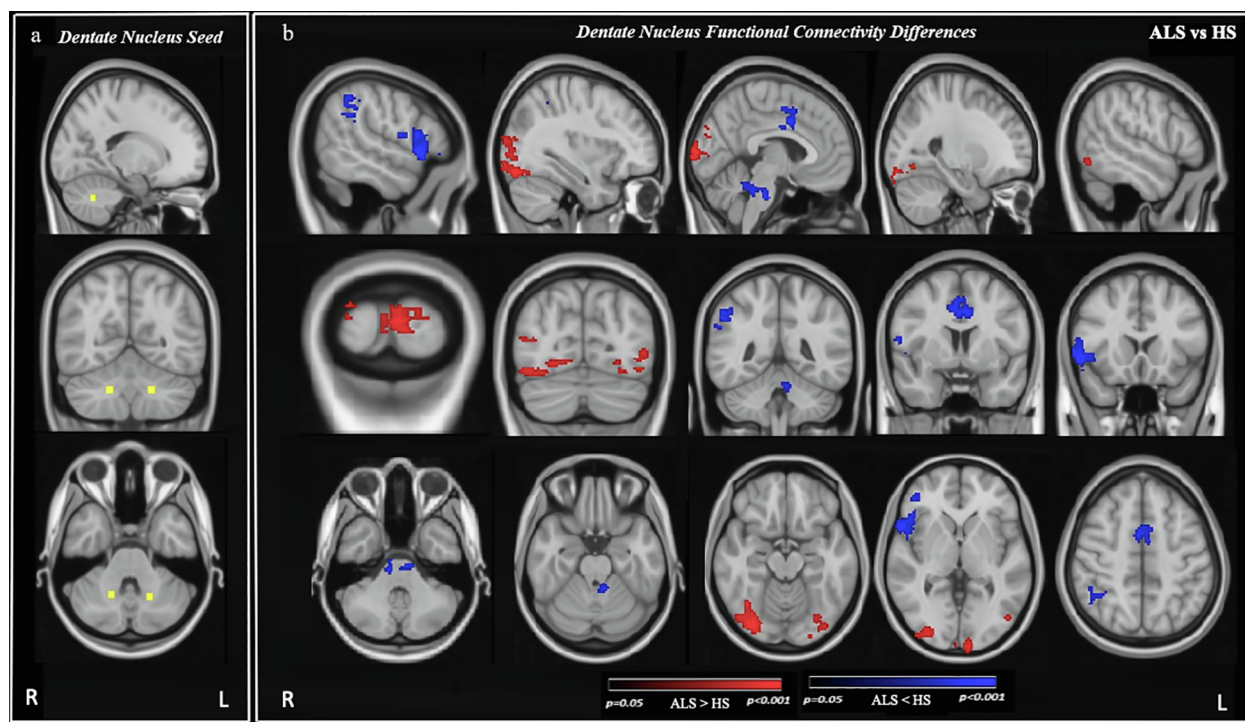


Fig. 1. Resting-state functional connectivity (rsFC) differences in the whole brain cerebral cortex between Amyotrophic Lateral Sclerosis (ALS) patients and healthy subjects (HS) obtained from the dentate nucleus (DN) as a seed. a: seed map of the DN (axial, sagittal, and coronal view). b: DN rsFC differences between ALS patients and HS (axial, sagittal, and coronal view). Yellow: DN seed. Red: Increased DN rsFC. Blue: Decreased DN rsFC. Results were corrected for the multiple comparisons at the family-wise error (FWE) of $p < 0.05$. Images are oriented in the radiological convention. (For interpretation of the references to colour in this figure legend, the reader is referred to the web version of this article.)

suggesting motor neuron degeneration consistent with decline in functional mobility of patients (Konrad et al., 2002; Agosta et al., 2011; Douaud et al., 2011; Luo et al., 2012; Chiò et al., 2014; Fang et al., 2016; Menke et al., 2016; Zhou et al., 2016; Qiu et al., 2019). Presumably in the current study, disrupted cerebello-cortical rsFC in ALS patients between cerebellar DN and motor cortex could be interpreted as dysfunctions in the cerebello-thalamo cortical pathways (Horne and Butler, 1995). The cerebello-thalamo cortical pathways play a critical role in skilled voluntary movements and motor adaptations (Horne and Butler, 1995). The pathways first originate in the deep cerebellar nuclei and then carry the cerebellar output signal from the cerebellum to the cerebral motor cortex via the SCP, bypassing the thalamus and contralateral red nucleus (Horne and Butler, 1995). One such pathway is the dentato-rubro-thalamo-cortical tract (Kwon et al., 2011; Khoyratty

and Wilson, 2013; Meola et al., 2016) which ascends from cerebellar DN to the primary and premotor cortex through the SCP (Asanuma et al., 1983; Horne and Butler, 1995; Dum and Strick, 2003; Akakin et al., 2014). In ALS, the exact connection of this pathway with the two brain structures has not been established yet and should be assessed in the future. However, anatomical alterations in such pathways were reported as an underlying cause of distorted cerebello-cortical rsFC in other neurodegenerative disorders i.e. Parkinson's disease, Freezing of Gait and Essential tremor (Pinto et al., 2003; Lenka et al., 2017; Bharti et al., 2019). Our findings are further supported by the positive correlation between the DN rsFC in the right precentral gyrus and left foot tapping scores of ALS patients. Tapping reflects clinical measurement of UMN burden dysfunction and thus lower tapping scores indicate worse motor status with impaired voluntary movements (Huynh et al., 2016).

Table 3

Brain areas exhibited altered cerebellar dentate nucleus resting-state functional connectivity.

Group Differences	Brain Areas	Clusters	Voxels			Coordinates	Peak z-stat
			X	Y	Z		
ALS > HS	Bilateral: Lateral occipital cortex, Occipital fusiform gyrus, Temporal occipital fusiform cortex, Occipital pole, Lingual gyrus, Supracalcarine cortex	1241 497 419	28 47 66	22 13 24	28 40 30	4.46 4.26 30.6	
ALS < HS	Right: Frontal pole, Inferior and middle frontal gyrus, Frontal and central operculum cortex, Frontal orbital cortex, Precentral and Postcentral gyrus, Supramarginal gyrus, Angular gyrus, Temporal pole. Left: Cerebellar lobule IV and Brain stem. Bilateral: Anterior cingulate cortex, and Supplementary motor area	849 459 459 452	16 44 48 12	70 52 65 45	35 19 54 51	4.74 3.36 3.71 3.63	

Coordinates were extracted from MNI 152 space.

ALS > HS represents higher whole brain resting-state functional connectivity with respect to dentate nucleus in ALS as compared to healthy subjects (HS). Results were corrected for family-wise error at $p < 0.05$ (FWE corrected; $p < 0.05$).

ALS < HS represents lower whole brain resting-state functional connectivity with respect to dentate nucleus in ALS as compared to healthy subjects (HS). Results were corrected for family-wise error at $p < 0.05$ (FWE corrected; $p < 0.05$).

*Peak z-stat denotes the maximum statistical value (z-stat) for the peak activity.

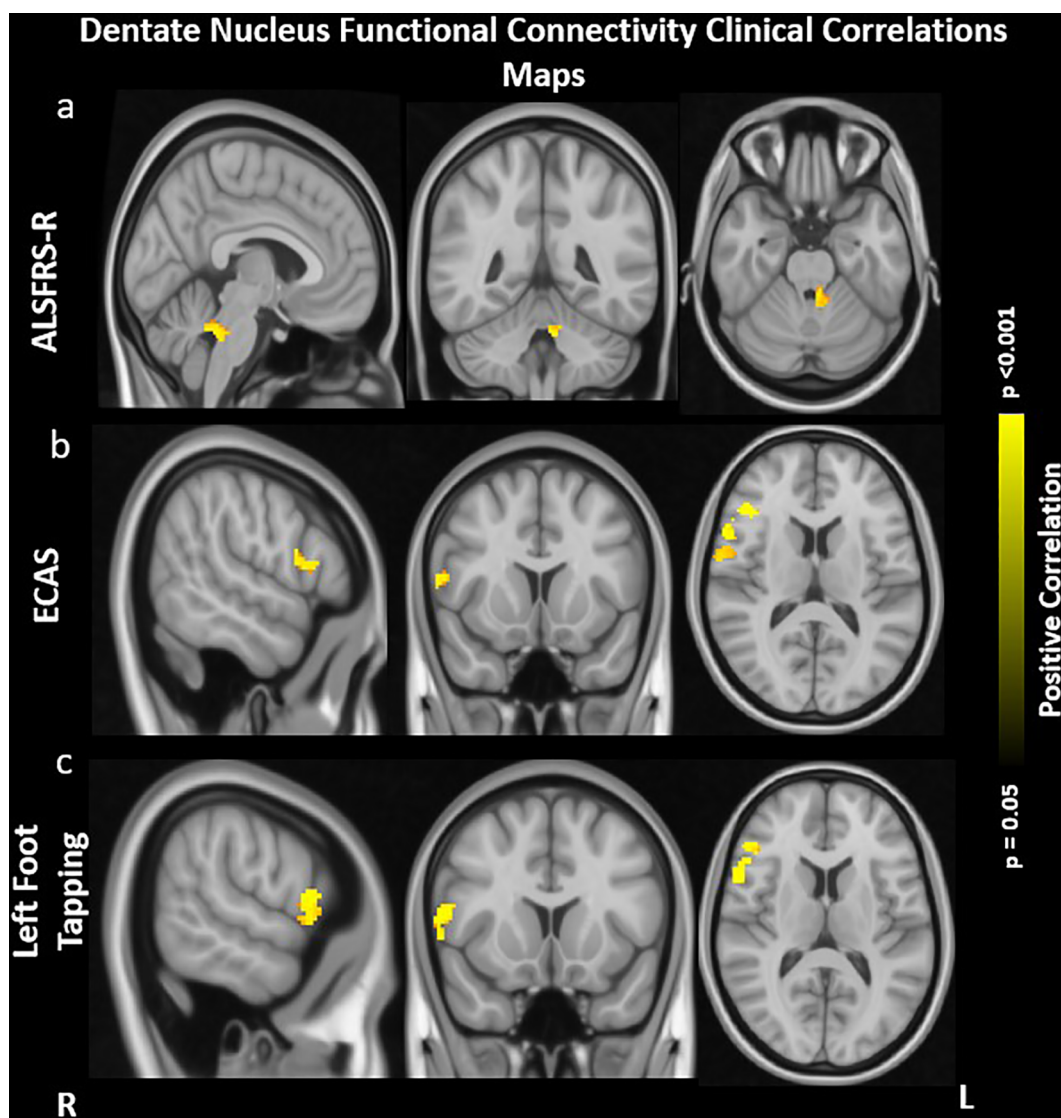


Fig. 2. Correlation Maps of Dentate Nucleus Functional Connectivity and Clinical Score. a: positive correlation between lower DN rsFC in left hemispheric lobule IV of cerebellum, brainstem and Amyotrophic Lateral Sclerosis Functional Rating Scale - Revised (ALSFRS-R). b: positive correlation between lower DN rsFC in right hemispheric inferior frontal gyrus, precentral gyrus, and anterior cingulate cortex with Edinburg cognitive and behavioral ALS screening (ECAS). c: positive correlation between lower DN rsFC in right hemispheric inferior frontal gyrus, precentral gyrus, and anterior cingulate cortex with left foot tapping. Results were obtained within the mask of rsFC differences in ALS patients and healthy subjects (HS). Results were corrected within these masks for multiple comparisons at the family-wise error (FWE) of $p < 0.05$. Images are oriented in radiological convention.

Since in ALS, UMN burden in the primary motor cortex is believed to degenerate first (Ragagnin et al., 2019), we hypothesize that abnormal cerebello-cortical rsFC between the DN and precentral gyrus is due to these anatomical alterations leading to a loss of motor functions and/or delay in the motor performances. Furthermore, a positive correlation was revealed between DN rsFC in the right precentral gyrus and ECAS scores. The ECAS is a clinical measurement of neuropsychological status (Niven et al., 2015), adjusting for motor impairment, and provides an overview of cognitive functioning in multiple domains including language, executive function, fluency in letters, memory and visuospatial functions (Abrahams et al., 2014). Lower ECAS scores indicate worsening of cognitive and behavioural performance (Abrahams et al., 2000, 2014). The correlation between the ECAS and DN-precentral gyrus rsFC is counter-intuitive as abnormalities in the precentral gyrus indicate worsening of motor functions (Kakei et al., 1999; Lemon, 2008). However, the precentral gyrus has also been shown to play a key role in maintaining other cognitive human functions such as regulating empathy, awareness, attention, and cognitive reappraisal (Cabeza and

Nyberg, 2000; Koechlin and Summerfield, 2007; Guo et al., 2012; Seo et al., 2014). Therefore, an association between the altered DN-precentral gyrus rsFC and ECAS scores may indicate a critical role of the precentral gyrus in maintaining cognitive functions.

4.2. rsFC between the DN and the subcortical brain regions

Another novel finding of this study is the lower rsFC between the DN and the subcortical brain structures (i.e. lobule IV of the cerebellum and brain stem) in ALS patients than in HS. Lobule IV of the cerebellum and brain stem plays a key role in controlling the motor system (Stoodley et al., 2012; Bede et al., 2019). Lobule IV of the cerebellum relates to the primary motor cortex and acts as a target brain region to consolidate demanding motor tasks (Kelly and Strick, 2003; Stoodley and Schmahmann, 2010; Stoodley et al., 2012). On the other hand, the brain stem acts as a hallmark to assess motor degeneration (Bede et al., 2019). Thus, deterioration of cerebellar DN rsFC with lobule IV and brain stem could indicate an alteration in the spinocerebellar tract. This

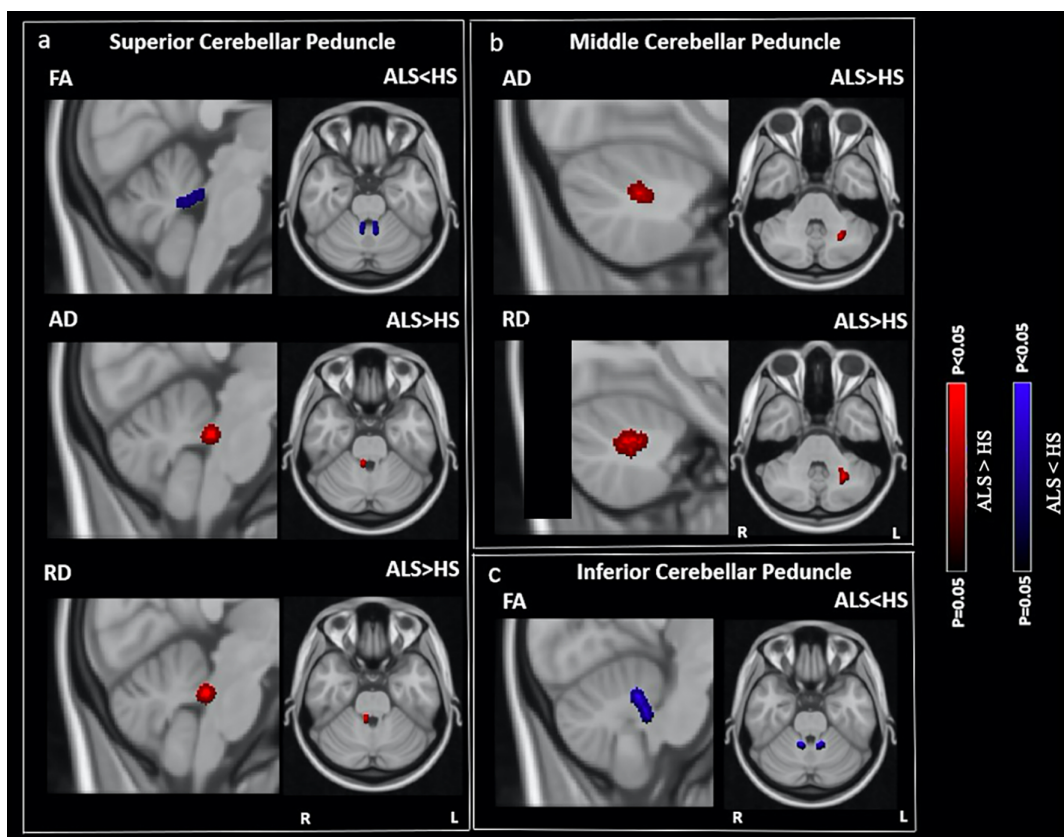


Fig. 3. Diffusion tensor imaging (DTI) differences in fractional anisotropy (FA), axial diffusivity (AD), and radial diffusivity (RD) between Amyotrophic Lateral Sclerosis (ALS) patients and healthy subjects (HS) at the superior cerebellar peduncle (SCP), middle cerebellar peduncle (MCP), and inferior cerebellar peduncle (ICP). a: lower FA, higher AD and RD in ALS patients than in HS at SCP. b: higher AD and RD in ALS patients than in HS at MCP. c: lower FA in ALS patients than in HS at ICP. Results were obtained within the mask of SCP, MCP, and ICP. Later, the DTI results were corrected for the multiple comparisons at the family-wise error (FWE) of $p < 0.05$. Blue: lower FA. Red: higher AD and RD. Images are oriented in radiological convention. (For interpretation of the references to colour in this figure legend, the reader is referred to the web version of this article.)

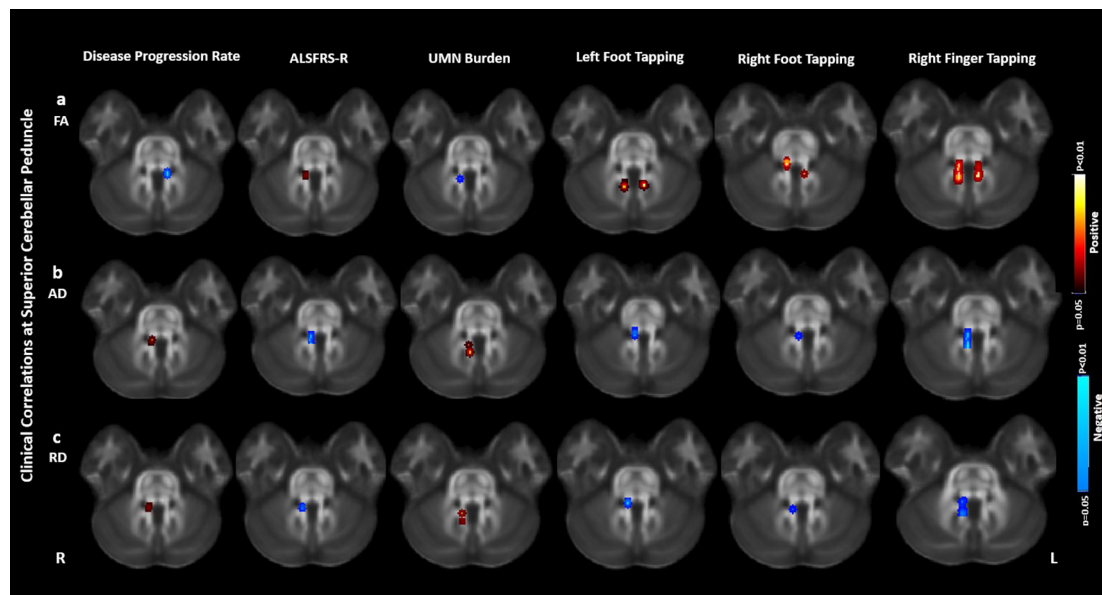


Fig. 4. Correlations of the DTI abnormalities at the superior cerebellar peduncle (SCP) with the clinical scores of Amyotrophic Lateral Sclerosis (ALS) patients. a: correlations of fractional anisotropy (FA) at the SCP with Amyotrophic Lateral Sclerosis Functional Rating Scale - Revised (ALSFRS-R), disease progression rate, upper motor neuron (UMN) burden, left foot tapping, right foot tapping, and right finger tapping scores. b: correlations of axial diffusivity (AD) at the SCP with ALSFRS-R, disease progression rate, UMN burden, left foot tapping, right foot tapping, and right finger tapping scores. c: correlations of radial diffusivity (RD) at the SCP with ALSFRS-R, disease progression rate, UMN burden, left foot tapping, right foot tapping, and right finger tapping scores. Blue: negative correlation. Red: positive correlation. The results were corrected for multiple comparisons at the false discovery rate (FDR) of $p < 0.05$. Images are oriented in radiological convention. (For interpretation of the references to colour in this figure legend, the reader is referred to the web version of this article.)

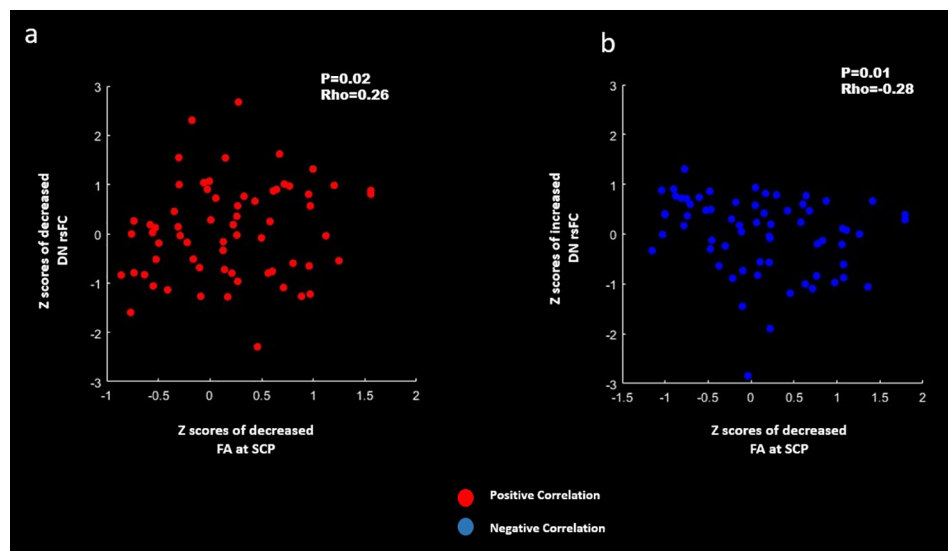


Fig. 5. Correlations between the z scores of dentate nucleus (DN) resting-state functional connectivity (rsFC) and findings of DTI parameters at the cerebellar peduncles of Amyotrophic Lateral Sclerosis (ALS) patients. a: positive correlation between lower DN rsFC and lower fractional anisotropy (FA) at the superior cerebellar peduncle (SCP) [P = 0.02; Rho = 0.26; Spearman Rank correlation]. b: negative correlation between higher DN rsFC and lower FA at the SCP [P = 0.01; Rho = -0.28; Spearman Rank correlation]. Red: Positive correlation. Blue: Negative correlation. Correlations results were corrected for a family-wise error (FWE) of p < 0.05. (For interpretation of the references to colour in this figure legend, the reader is referred to the web version of this article.)

particular tract carries afferent fibers that ascend from the medulla and pons to the DN through lobule IV via ICP and thus plays a key role in maintaining the balance, posture and equilibrium (Akakin et al., 2014; Gebrek et al., 2014). Therefore, the findings indicate motor relevance of disrupted rsFC between DN and subcortical structures (i.e. lobule IV and brain stem). Furthermore, a positive correlation was revealed with ALSFRS-R, suggesting that an association between DN subcortical rsFC and ALS disease severity represents the underlying pathophysiology of ALS.

4.3. rsFC between the DN and the extra-motor brain regions

Another interesting finding of the current study is the lower rsFC between the DN and several other extra-motor brain areas (i.e. frontal, prefrontal, temporal, and postcentral gyrus) of ALS patients than HS. Functional involvement of these areas in ALS has been previously studied and suggests that ALS pathology extends beyond motor control (Mohammadi et al., 2009; Luo et al., 2012; Agosta et al., 2013; Chiò et al., 2014; Zhou et al., 2016; Loewe et al., 2017). One plausible explanation for higher neurodegeneration in these areas with respect to DN connectivity could be an alteration in the anatomical projections from the DN to frontal, prefrontal and posterior parietal brain regions, as suggested previously (Salamon et al., 2007; Suzuki et al., 2012). The abnormal functional cerebral connections with respect to DN could be due to the alterations in the contralateral cerebello-thalamo-cortical pathways. This suggests that anatomical alterations in the dentato-rubro-thalamo-cortical tract directing efferent fibers from the DN to the cerebral cortex through SCP are likely involved in the disrupted connections between the DN and extra-motor brain regions. No neuroimaging study so far has investigated the role of these pathways in ALS and additional research is required in this area. However, the output of DN acts as an anatomical substrate for not only controlling skilled voluntary movements but also cognition, behaviour, and higher executive functions in primates (Dum et al., 2002). Furthermore, a positive correlation was observed between the lower DN rsFC in the right inferior frontal gyrus and right anterior cingulate gyrus with the ECAS and left foot tapping scores. Because the dentato-rubro-thalamo-cortical projections from the DN terminate in the motor, frontal, prefrontal, and posterior parietal brain regions (Dum et al., 2002), the finding of strong associations with worse motor and cognitive performances confirms a fundamental role of the dentato-rubro-thalamo-cortical tract in regulating both motor and extra-motor functions. Secondly, it has been previously hypothesized that ALS motor and cognitive abnormalities are associated with network dysfunctions with the cerebellum, frontal,

temporal, and posterior parietal brain regions (Mohammadi et al., 2009; Agosta et al., 2011, 2013; Luo et al., 2012; Chiò et al., 2014; Zhou et al., 2016; Loewe et al., 2017; Qiu et al., 2019). In agreement with these studies, the current findings suggest that the functional interaction between these complex brain circuits result in motor and cognitive decline in ALS. In contrast, we also observed higher DN rsFC in the cortical extra-motor brain areas of the cerebral cortex (occipital pole, lateral occipital cortex, temporal occipital fusiform cortex, occipital fusiform gyrus, lingual gyrus, and supracalcarine cortex). One plausible explanation of the increased rsFC between the DN and parieto-occipital brain regions could be a compensatory response mechanism for the reduced DN rsFC with the other motor and extra-motor brain regions (i.e. the motor, frontal, prefrontal and temporal). In addition, higher synchronization of BOLD signals could be due to the loss of inhibitory interneurons or a disease-related adaptive response (Hillary et al., 2015). An alternative explanation could be functional reorganization of parieto-occipital brain regions in ALS patients in response to the disease (Hillary et al., 2015).

4.4. WM diffusivity at the cerebellar peduncles

The WM findings of lower FA at the SCP and ICP, and higher AD and RD at the SCP and MCP, were observed in ALS patients when compared to HS. In humans, the SCP consists of efferent fibers which anatomically connect the DN and the cerebral cortex through the thalamus and the contralateral red nucleus via cerebello-thalamo-cortical pathways (Behrens et al., 2003; Salamon et al., 2007; Haines and Dietrichs, 2012). Therefore, alterations in FA, AD, and RD at SCP, may likely indicate damage in the efferent pathways passing from the DN to the cortex through cerebello-thalamo-cortical pathways (Granziera et al., 2009; Palesi et al., 2015). Similarly, MCP and ICP consist of afferent fibers which anatomically connect the cerebral cortex to the cerebellum through the pons and brain stem (Haines and Dietrichs, 2012). The lower FA at ICP and higher AD and RD at MCP may indicate structural disconnection of the DN with not only supratentorial brain structures but also with infratentorial brain structures (Granziera et al., 2009; Palesi et al., 2015) suggesting changes in the afferent pathways through cerebello-thalamo-cortical loops and spinocerebellar loops. To our surprise, loss of fiber integrity in all the three cerebellar peduncles (i.e. the SCP, MCP and ICP) significantly correlated with ALSFRS-R, symptom duration, and disease progression rate. The findings are in agreement with overall characteristics of ALS suggesting that as the disease progresses, the WM degeneration at the cerebellar peduncles increases and in turn worsens clinical symptoms. Moreover,

microstructural WM damage in all the three cerebellar peduncles correlated with UMN burden scores and tapping scores. Keeping with the progressive nature of ALS, the clinical correlations with UMN burden scores and tapping scores clearly indicates that WM degeneration at the pathways connecting the DN and supra- and infra-tentorial brain structures is associated with overall disease burden.

So far, no study has explored these abnormalities using the cerebellar peduncles. Previous studies have examined WM abnormalities in the whole cerebellum rather than cerebellar peduncles, corticospinal tract, corpus callosum and extra-motor brain regions (Thivard et al., 2007; Verstraete et al., 2010; Canu et al., 2011; Cirillo et al., 2012; Trojsi et al., 2015; Femiano et al., 2018; Bede et al., 2015). Unlike other studies (Tan et al., 2014), we did not find GM atrophy in any of the cerebellar lobules. Our cohort may be more reflective of the broader ALS population due to our increased sample size and multiple sites of data acquisition. Therefore, the contradictory findings may be due to the high variability in the sample size, acquisition parameters, and different analytical methodologies in other studies.

4.5. Correlations between the DN rsFC and DTI findings

Lastly, we found significant correlations between DN rsFC and FA at the SCP. Damage to the efferent fibers carried by the SCP connecting the cerebellar DN to the cerebral cortex via the thalamus (Haines and Dietrichs, 2012) and contralateral red nucleus through dentato-rubrothalamic tract (Kwon et al., 2011; Meola et al., 2016) is possibly involved in the pathophysiology of ALS. Thus, we speculate that degeneration at the SCP could have contributed to the altered DN rsFC: i.e. abnormal DN rsFC is a major representative of structural alterations in the WM.

4.6. Conclusion

The novelty of our study is to examine both structural and functional aberrations of the cerebellar DN using multimodal MRI including rs-fMRI, DTI and volumetric analysis using SUIT in patients with ALS and HS. Overall, the study suggests that abnormal cerebellar DN structural and functional connectivity is involved in the pathophysiological mechanism of ALS. The correlations between DN rsFC and clinical data such as the ALSFRS-R, disease progression rate, ECAS, UMN burden and tapping scores emphasize the relevance of abnormal cerebellar connectivity patterns extending beyond motor brain regions to extra-motor brain areas. The findings thus suggest rsFC abnormalities are associated with cerebellar DN and its associated WM fiber tracts in ALS disease. Moreover, the clinical correlations between abnormal cerebellar DN rsFC and FA at SCP suggest cerebellar peduncular WM degeneration contributes to dentato-cerebral dysfunction. One limitation of the current study arises from MRI data acquisition using multiple imaging systems and sites which may contribute to the possible chances of error in the statistical differences. However, a harmonized imaging protocol was used across the sites and we have performed statistical analysis using multiple linear regression models in FSL by carefully regressing out the effect of age, gender, MRI scanners, site of data acquisition and motion parameters. Thus, keeping aside cerebellar volumetric results, altered DN cerebellar rsFC and the corresponding WM changes in all three cerebellar peduncles may have contributed in the pathophysiology of ALS. Future longitudinal study at different time points could better explain the involvement of cerebellar DN in ALS pathology and the changes in brain plasticity that occur over time.

Declaration of Competing Interest

The authors declare that they have no known competing financial interests or personal relationships that could have appeared to influence the work reported in this paper.

Acknowledgements

This study was funded by the Canadian Institutes of Health Research (CIHR), the ALS Society of Canada, Brain Canada Foundation, Shelly Mrkonjic Research Fund. Data management and quality control was facilitated by the Canadian Neuromuscular Disease Registry.

Data and code availability statement

All data used for this study are stored at the Department of Medicine of University of Alberta. Any data and code associated with this original research article will be made available by reasonable request to corresponding author (SK).

References

- Abrahams, S., Leigh, P.N., Harvey, A., Vythelingum, G.N., Grisé, D., Goldstein, L.H., 2000. Verbal fluency and executive dysfunction in amyotrophic lateral sclerosis (ALS). *Neuropsychologia* 38, 734–747.
- Abrahams, S., Newton, J., Niven, E., Foley, J., Bak, T.H., 2014. Screening for cognition and behaviour changes in ALS. *Amyotroph. Lateral Scler. Front. Degener.* 15, 9–14.
- Agosta, F., Canu, E., Valsasina, P., Riva, N., Prelle, A., Comi, G., Filippi, M., 2013. Divergent brain network connectivity in amyotrophic lateral sclerosis. *Neurobiol. Aging* 34, 419–427.
- Agosta, F., Pagani, E., Rocca, M.A., Caputo, D., Perini, M., Salvi, F., Prelle, A., Filippi, M., 2007. Voxel-based morphometry study of brain volumetry and diffusivity in amyotrophic lateral sclerosis patients with mild disability. *Hum. Brain Mapp.* 28, 1430–1438.
- Agosta, F., Valsasina, P., Absinta, M., Riva, N., Sala, S., Prelle, A., Copetti, M., Comola, M., Comi, G., Filippi, M., 2011. Sensorimotor functional connectivity changes in amyotrophic lateral sclerosis. *Cereb. Cortex* 21, 2291–2298.
- Agosta, F., Valsasina, P., Riva, N., Copetti, M., Messina, M.J., Prelle, A., Comi, G., Filippi, M., 2012. The cortical signature of amyotrophic lateral sclerosis. *PLOS One* 7, e42816.
- Akakin, A., Peris-Celda, M., Kilic, T., Seker, A., Gutierrez-Martin, A., Rhoton, A., 2014. The dentate nucleus and its projection system in the human cerebellum—the dentate nucleus microsurgical anatomical study. *Neurosurgery* 74, 401–425.
- Alonso, A., Logroscino, G., Jick, S.S., Hernán, M.A., 2009. Incidence and lifetime risk of motor neuron disease in the United Kingdom: a population-based study. *Eur. J. Neurol.* 16, 745–751.
- Ananuma, C., Thach, W.T., Jones, E.G., 1983. Distribution of cerebellar terminations and their relation to other afferent terminations in the ventral lateral thalamic region of the monkey. *Brain Res. Rev.* 5, 237–265.
- Bede, P., Chipika, R.H., Finegan, E., Li Hi Shing, S., Doherty, M.A., Hengeveld, J.C., Vajda, A., Hutchinson, S., Donaghy, C., McLaughlin, R.L., Hardiman, O., 2019. Brainstem pathology in amyotrophic lateral sclerosis and primary lateral sclerosis: a longitudinal neuroimaging study. *NeuroImage Clin.* 24.
- Bede, P., Elamin, M., Byrne, S., McLaughlin, R.L., Kenna, K., Vajda, A., Fagan, A., Bradley, D.G., Hardiman, O., 2015. Patterns of cerebral and cerebellar white matter degeneration in ALS. *J. Neurol. Neurosurg. Psychiatry* 86, 468–470.
- Beghi, E., Logroscino, G., Chiò, A., Hardiman, O., Mitchell, D., Swingler, R., Traynor, B.J., EURALS Consortium, 2006. The epidemiology of ALS and the role of population-based registries. *Biochim. Biophys. Acta* 1762, 1150–1157.
- Behrens, T.E.J., Johansen-Berg, H., Woolrich, M.W., Smith, S.M., Wheeler-Kingshott, C.A.M., Bouly, P.A., Barker, G.J., Sillery, E.L., Sheehan, K., Ciccarelli, O., Thompson, A.J., Brady, J.M., Matthews, P.M., 2003. Non-invasive mapping of connections between human thalamus and cortex using diffusion imaging. *Nat. Neurosci.* 6, 750–757.
- Bernard, J.A., Peltier, S.J., Benson, B.L., Wiggins, J.L., Jaeggi, S.M., Buschkuhl, M., Jonides, J., Monk, C.S., Seidler, R.D., 2014. Dissociable functional networks of the human dentate nucleus. *Cereb. Cortex* 24, 2151–2159.
- Bharti, K., Suppa, A., Pietracupa, S., Upadhyay, N., Gianni, C., Leodori, G., Di Biasio, F., Modugno, N., Petsas, N., Grillea, G., Zampogna, A., Berardelli, A., Pantano, P., 2019. Abnormal cerebellar connectivity patterns in patients with parkinson's disease and freezing of gait. *Cerebellum* 18, 298–308.
- Biswal, B.B., Yetkin, F.Z., Haughton, V.M., Hyde, J.S., 1995. Functional connectivity in the motor cortex of resting human brain using echo-planar MRI. *Magn. Reson. Med.* 34, 537–541.
- Biswal, B.B., 2012. Resting state fMRI: a personal history. *NeuroImage*, 20 YEARS OF fMRI20 YEARS OF fMRI. 62, 938–944.
- Brazis, P.W., Biller, J., Fine, M., Palacios, E., Pagano, R.J., 1981. Cerebellar degeneration with Hodgkin's disease: computed tomographic correlation and literature review. *Arch. Neurol.* 38, 253–256.
- Brooks, B.R., 1994. El Escorial World Federation of Neurology criteria for the diagnosis of amyotrophic lateral sclerosis. Subcommittee on Motor Neuron Diseases/Amyotrophic Lateral Sclerosis of the World Federation of Neurology Research Group on Neuromuscular Diseases and the El Escorial "Clinical limits of amyotrophic lateral sclerosis" workshop contributors. *J. Neurol. Sci.* 124 (Suppl), 96–107.
- Buckner, R.L., 2013. The brain's default network: origins and implications for the study of psychosis. *Dialogues Clin. Neurosci.* 15, 351–358.
- Cabeza, R., Nyberg, L., 2000. Imaging cognition II: an empirical review of 275 PET and

- fMRI studies. *J. Cogn. Neurosci.* 12, 1–47.
- Canu, E., Agosta, F., Riva, N., Sala, S., Prelle, A., Caputo, D., Perini, M., Comi, G., Filippi, M., 2011. The topography of brain microstructural damage in amyotrophic lateral sclerosis assessed using diffusion tensor MR imaging. *Am. J. Neuroradiol.* 32, 1307–1314.
- Cedarbaum, J.M., Stambler, N., Malta, E., Fuller, C., Hilt, D., Thurmond, B., Nakanishi, A., 1999. The ALSFRS-R: a revised ALS functional rating scale that incorporates assessments of respiratory function. BDNF ALS Study Group (Phase III). *J. Neurol. Sci.* 169, 13–21.
- Chan-Palay, V., Palay, S.L., Brown, J.T., Van Itallie, C., 1977. Sagittal organization of olivocerebellar and reticulocerebellar projections: autoradiographic studies with 35S-methionine. *Exp. Brain Res.* 30, 561–576.
- Chenji, S., Jha, S., Lee, D., Brown, M., Seres, P., Mah, D., Kalra, S., 2016. Investigating default mode and sensorimotor network connectivity in amyotrophic lateral sclerosis. *PLoS One* 11.
- Chiò, A., Pagani, M., Agosta, F., Calvo, A., Cistaro, A., Filippi, M., 2014. Neuroimaging in amyotrophic lateral sclerosis: insights into structural and functional changes. *Lancet Neurol.* 13, 1228–1240.
- Cirillo, M., Esposito, F., Tedeschi, G., Caiazzo, G., Sagnelli, A., Piccirillo, G., Conforti, R., Tortora, F., Monsurrò, M.R., Cirillo, S., Trojsi, F., 2012. Widespread microstructural white matter involvement in amyotrophic lateral sclerosis: a whole-brain DTI study. *AJNR Am. J. Neuroradiol.* 33, 1102–1108.
- del Aguila, M.A., Longstreth, W.T., McGuire, V., Koepsell, T.D., van Belle, G., 2003. Prognosis in amyotrophic lateral sclerosis: a population-based study. *Neurology* 60, 813–819.
- Diedrichsen, J., 2006. A spatially unbiased atlas template of the human cerebellum. *NeuroImage* 33, 127–138.
- Diedrichsen, J., Maderwald, S., Küper, M., Thürling, M., Rabe, K., Gizewski, E.R., Ladd, M.E., Timmann, D., 2011. Imaging the deep cerebellar nuclei: a probabilistic atlas and normalization procedure. *NeuroImage* 54, 1786–1794.
- Douaud, G., Filippini, N., Knight, S., Talbot, K., Turner, M.R., 2011. Integration of structural and functional magnetic resonance imaging in amyotrophic lateral sclerosis. *Brain* 134, 3470–3479.
- Dun, R.P., Li, C., Strick, P.L., 2002. Motor and nonmotor domains in the monkey dentate. *Ann. N. Y. Acad. Sci.* 978, 289–301.
- Dun, R.P., Strick, P.L., 2003. An unfolded map of the cerebellar dentate nucleus and its projections to the cerebral cortex. *J. Neurophysiol.* 89, 634–639.
- Easterling, C., Antinoja, J., Cashin, S., Barkaus, P.E., 2013. Changes in tongue pressure, pulmonary function, and salivary flow in patients with amyotrophic lateral sclerosis. *Dysphagia* 28, 217–225.
- Fang, X., Zhang, Y., Wang, Y., Zhang, Y., Hu, J., Wang, J., Zhang, J., Jiang, T., 2016. Disrupted effective connectivity of the sensorimotor network in amyotrophic lateral sclerosis. *J. Neurol.* 263, 508–516.
- Fasano, A., Laganier, S.E., Lam, S., Fox, M.D., 2017. Lesions causing freezing of gait localize to a cerebellar functional network. *Ann. Neurol.* 81, 129–141.
- Femiano, C., Trojsi, F., Caiazzo, G., Siciliano, M., Passaniti, C., Russo, A., Biscecco, A., Cirillo, M., Monsurrò, M.R., Esposito, F., Tedeschi, G., Santangelo, G., 2018. Apathy is correlated with widespread diffusion tensor imaging (DTI) impairment in amyotrophic lateral sclerosis [WWW Document]. *Behav. Neurol.* <https://www.hindawi.com/journals/bn/2018/2635202/>.
- Ferraro, P.M., Agosta, F., Riva, N., Copetti, M., Spinelli, E.G., Falzone, Y., Soraru, G., Comi, G., Chiò, A., Filippi, M., 2017. Multimodal structural MRI in the diagnosis of motor neuron diseases. *NeuroImage Clin.* 16, 240–247.
- Gavrilescu, M., Shaw, M.E., Stuart, G.W., Eckersley, P., Svalbe, I.D., Egan, G.F., 2002. Simulation of the effects of global normalization procedures in functional MRI. *NeuroImage* 17, 532–542.
- Geborek, P., Bengtsson, F., Jörntell, H., 2014. Properties of bilateral spinocerebellar activation of cerebellar cortical neurons. *Front. Neural Circ.* 8, 128.
- Geser, F., Brandmeir, N.J., Kwong, L.K., Martinez-Lage, M., Elman, L., McCluskey, L., Xie, S.X., Lee, V.M.-Y., Trojanowski, J.Q., 2008. Evidence of multisystem disorder in whole-brain map of pathological TDP-43 in amyotrophic lateral sclerosis. *Arch. Neurol.* 65, 636–641.
- Goldstein, L.H., Abrahams, S., 2013. Changes in cognition and behaviour in amyotrophic lateral sclerosis: nature of impairment and implications for assessment. *Lancet Neurol.* 12, 368–380.
- Granziera, C., Schmahmann, J.D., Hadjikhani, N., Meyer, H., Meuli, R., Wedeen, V., Krueger, G., 2009. Diffusion spectrum imaging shows the structural basis of functional cerebellar circuits in the human cerebellum *in vivo*. *PLOS One* 4, e5101.
- Guo, X., Zheng, L., Zhang, W., Zhu, L., Li, J., Wang, Q., Dienes, Z., Yang, Z., 2012. Empathic neural responses to others' pain depend on monetary reward. *Soc. Cogn. Affect. Neurosci.* 7, 535–541.
- Haines, D.E., Dietrichs, E., 2012. The cerebellum – structure and connections. *Handb Clin. Neurol.* 103, 3–36.
- Hardiman, O., van den Berg, L.H., Kiernan, M.C., 2011. Clinical diagnosis and management of amyotrophic lateral sclerosis. *Nat. Rev. Neurol.* 7, 639–649.
- Heimrath, J., Gorges, M., Kassubek, J., Müller, H.-P., Birbaumer, N., Ludolph, A.C., Lulé, D., 2014. Additional resources and the default mode network: evidence of increased connectivity and decreased white matter integrity in amyotrophic lateral sclerosis. *Amyotroph. Lateral Scler. Front. Degener.* 15, 537–545.
- Hillary, F.G., Roman, C.A., Venkatesan, U., Rajtmajer, S.M., Bajaj, R., Castellanos, N.D., 2015. Hyperconnectivity is a fundamental response to neurological disruption. *Neuropsychology* 29, 59–75.
- Hoover, J.E., Strick, P.L., 1999. The organization of cerebellar and basal ganglia outputs to primary motor cortex as revealed by retrograde transneuronal transport of herpes simplex virus type 1. *J. Neurosci. J. Soc. Neurosci.* 19, 1446–1463.
- Horne, M.K., Butler, E.G., 1995. The role of the cerebello-thalamo-cortical pathway in skilled movement. *Prog. Neurobiol.* 46, 199–213.
- Huynh, W., Simon, N.G., Grosskreutz, J., Turner, M.R., Vucic, S., Kiernan, M.C., 2016. Assessment of the upper motor neuron in amyotrophic lateral sclerosis. *Clin. Neurophysiol.* 127, 2643–2660.
- Jelsone-Swain, L.M., Fling, B.W., Seidler, R.D., Hovatter, R., Gruis, K., Welsh, R.C., 2010. Reduced interhemispheric functional connectivity in the motor cortex during rest in limb-onset amyotrophic lateral sclerosis. *Front. Syst. Neurosci.* 4, 158.
- Jenkinson, M., Beckmann, C.F., Behrens, T.E.J., Woolrich, M.W., Smith, S.M., 2012. FSL. *NeuroImage* 62, 782–790.
- Kakei, S., Hoffman, D.S., Strick, P.L., 1999. Muscle and movement representations in the primary motor cortex. *Scienc.* 285, 2136–2139.
- Kassubek, J., Unrath, A., Huppertz, H.-J., Lulé, D., Ethofer, T., Sperfeld, A.-D., Ludolph, A.C., 2005. Global brain atrophy and corticospinal tract alterations in ALS, as investigated by voxel-based morphometry of 3-D MRI. *Amyotroph. Lateral Scler. Mot. Neuron Disord. Off. Publ. World Fed. Neurol. Res. Group Mot. Neuron Dis.* 6, 213–220.
- Kelly, R.M., Strick, P.L., 2003. Cerebellar loops with motor cortex and prefrontal cortex of a nonhuman primate. *J. Neurosci.* 23, 8432–8444.
- Khoiratty, F., Wilson, T., 2013. The dentato-rubro-olivary tract: clinical dimension of this anatomical pathway [WWW Document]. *Case Rep. Otolaryngol.* <https://www.hindawi.com/journals/criot/2013/934386/>.
- Kimura, F., Fujimura, C., Ishida, S., Nakajima, H., Furutama, D., Uehara, H., Shinoda, K., Sugino, M., Hanafusa, T., 2006. Progression rate of ALSFRS-R at time of diagnosis predicts survival time in ALS. *Neurology* 66, 265–267.
- Koechlin, E., Summerfield, C., 2007. An information theoretical approach to prefrontal executive function. *Trends Cogn. Sci.* 11, 229–235.
- Konrad, C., Henningsen, H., Bremer, J., Mock, B., Deppe, M., Buchinger, C., Turski, P., Knecht, S., Brooks, B., 2002. Pattern of cortical reorganization in amyotrophic lateral sclerosis: a functional magnetic resonance imaging study. *Exp. Brain Res.* 143, 51–56.
- Kozioł, L.F., Budding, D., Andreassen, N., D'Arrigo, S., Bulgheroni, S., Imamizu, H., Ito, M., Manto, M., Marvel, C., Parker, K., Pezzulo, G., Ramnani, N., Riva, D., Schmahmann, J., Vandervert, L., Yamazaki, T., 2014. Consensus paper: the cerebellum's role in movement and cognition. *Cerebellum Lond. Engl.* 13, 151–177.
- Kwon, H.G., Hong, J.H., Hong, C.P., Lee, D.H., Ahn, S.H., Jang, S.H., 2011. Dentatorubrothalamic tract in human brain: diffusion tensor tractography study. *Neuroradiology* 53, 787–791.
- Lemon, R.N., 2008. Descending pathways in motor control. *Annu. Rev. Neurosci.* 31, 195–218.
- Lenka, A., Bhalsing, K.S., Panda, R., Jhunjhunwala, K., Naduthota, R.M., Saini, J., Bharath, R.D., Yadav, R., Pal, P.K., 2017. Role of altered cerebello-thalamo-cortical network in the neurobiology of essential tremor. *Neuroradiolog.* 59, 157–168.
- Loewe, K., Machts, J., Kaufmann, J., Petri, S., Heinze, H.-J., Borgelt, C., Harris, J.A., Vielhaber, S., Schoenfeld, M.A., 2017. Widespread temporo-occipital lobe dysfunction in amyotrophic lateral sclerosis. *Sci. Rep.* 7.
- Luo, C., Chen, Q., Huang, R., Chen, X., Chen, K., Huang, X., Tang, H., Gong, Q., Shang, H.-F., 2012. Patterns of spontaneous brain activity in amyotrophic lateral sclerosis: a resting-state fMRI study. *PloS One* 7, e45470.
- Macey, P.M., Macey, K.E., Kumar, R., Harper, R.M., 2004. A method for removal of global effects from fMRI time series. *NeuroImage* 22, 360–366.
- Maknojia, S., Churchill, N.W., Schweizer, T.A., Graham, S.J., 2019. Resting state fMRI: going through the motions. *Front. Neurosci.* 13.
- Menke, R.A.L., Proudfoot, M., Talbot, K., Turner, M.R., 2017. The two-year progression of structural and functional cerebral MRI in amyotrophic lateral sclerosis. *NeuroImage Clin.* 17, 953–961.
- Menke, R.A.L., Proudfoot, M., Wuu, J., Andersen, P.M., Talbot, K., Benatar, M., Turner, M.R., 2016. Increased functional connectivity common to symptomatic amyotrophic lateral sclerosis and those at genetic risk. *J. Neurol. Neurosurg. Psychiatry* 87, 580–588.
- Meola, A., Comert, A., Yeh, F.-C., Sivakanthan, S., Fernandez-Miranda, J.C., 2016. The nondecussating pathway of the dentatorubrothalamic tract in humans: human connectome-based tractographic study and microdissection validation. *J. Neurosurg.* 124, 1406–1412.
- Middleton, F.A., Strick, P.L., 1996. Basal ganglia and cerebellar output influences non-motor function. *Mol. Psychiatry* 1, 429–433.
- Middleton, F.A., Strick, P.L., 2000. Basal ganglia and cerebellar loops: motor and cognitive circuits. *Brain Res. Rev.* 31, 236–250.
- Middleton, F.A., Strick, P.L., 2001. Cerebellar projections to the prefrontal cortex of the primate. *J. Neurosci.* 21, 700–712.
- Moberget, T., Ivry, R.B., 2019. Prediction, psychosis, and the cerebellum. *Biol. Psychiatry Cogn. Neurosci. Neuroimag.* 4, 820–831.
- Mochizuki, Y., Isozaki, E., Takao, M., Hashimoto, T., Shibuya, M., Arai, M., Hosokawa, M., Kawata, A., Oyanagi, K., Mihara, B., Mizutani, T., 2012. Familial ALS with FUS P525L mutation: two Japanese sisters with multiple systems involvement. *J. Neurol. Sci.* 323, 85–92.
- Mohammadi, B., Kollewe, K., Samii, A., Krampf, K., Dengler, R., Münte, T.F., 2009. Changes of resting state brain networks in amyotrophic lateral sclerosis. *Exp. Neurol.* 217, 147–153.
- Mormina, E., Petracca, M., Bommarito, G., Piaggio, N., Cocozza, S., Inglese, M., 2017. Cerebellum and neurodegenerative diseases: beyond conventional magnetic resonance imaging. *World J. Radiol.* 9, 371–388.
- Nakano, T., Nakaso, K., Nakashima, K., Ohama, E., 2004. Expression of ubiquitin-binding protein p62 in ubiquitin-immunoreactive intraneuronal inclusions in amyotrophic lateral sclerosis with dementia: analysis of five autopsy cases with broad clinicopathological spectrum. *Acta Neuropathol. (Berl.)* 107, 359–364.
- Niven, E., Newton, J., Foley, J., Colville, S., Swingler, R., Chandran, S., Bak, T.H., Abrahams, S., 2015. Validation of the Edinburgh cognitive and behavioural

- amyotrophic lateral sclerosis screen (ECAS): a cognitive tool for motor disorders. *Amyotroph. Lateral Scler. Front. Degener.* 16, 172–179.
- Palesi, F., Tournier, J.-D., Calamante, F., Muhlert, N., Castellazzi, G., Chard, D., D'Angelo, E., Wheeler-Kingshott, C.A.M., 2015. Contralateral cerebello-thalamo-cortical pathways with prominent involvement of associative areas in humans *in vivo*. *Brain Struct. Funct.* 220, 3369–3384.
- Phukan, J., Elamin, M., Bede, P., Jordan, N., Gallagher, L., Byrne, S., Lynch, C., Pender, N., Hardiman, O., 2012. The syndrome of cognitive impairment in amyotrophic lateral sclerosis: a population-based study. *J. Neurol. Neurosurg. Psychiatry* 83, 102–108.
- Phukan, J., Pender, N.P., Hardiman, O., 2007. Cognitive impairment in amyotrophic lateral sclerosis. *Lancet Neurol.* 6, 994–1003.
- Pinto, A.D., Lang, A.E., Chen, R., 2003. The cerebellothalamic pathway in essential tremor. *Neurology* 60, 1985–1987.
- Qiu, T., Zhang, Y., Tang, X., Liu, X., Wang, Y., Zhou, C., Luo, C., Zhang, J., 2019. Precentral degeneration and cerebellar compensation in amyotrophic lateral sclerosis: a multimodal MRI analysis. *Hum. Brain Mapp.* 40, 3464–3474.
- Ragagnin, A.M.G., Shadfar, S., Vidal, M., Jamali, M.S., Atkin, J.D., 2019. Motor neuron susceptibility in ALS/FTD. *Front. Neurosci.* 13.
- Rowland, L.P., Shneider, N.A., 2001. Amyotrophic lateral sclerosis. *N. Engl. J. Med.* 344, 1688–1700.
- Salamon, N., Sicotte, N., Drain, A., Frew, A., Alger, J.R., Jen, J., Perlman, S., Salamon, G., 2007. White matter fiber tractography and color mapping of the normal human cerebellum with diffusion tensor imaging. *J. Neuroradiol. J. Neuroradiol.* 34, 115–128.
- Schmahmann, J.D., Sherman, J.C., 1998. The cerebellar cognitive affective syndrome. *Brain J. Neurol.* 121 (Pt 4), 561–579.
- Seo, D., Olman, C.A., Haut, K.M., Sinha, R., MacDonald, A.W., Patrick, C.J., 2014. Neural correlates of preparatory and regulatory control over positive and negative emotion. *Soc. Cogn. Affect. Neurosci.* 9, 494–504.
- Shen, D., Hou, B., Xu, Y., Cui, B., Peng, P., Li, X., Tai, H., Zhang, K., Liu, S., Fu, H., Gao, J., Liu, M., Feng, F., Cui, L., 2018. Brain structural and perfusion signature of amyotrophic lateral sclerosis with varying levels of cognitive deficit. *Front. Neurol.* 9.
- Smith, S.M., Fox, P.T., Miller, K.L., Glahn, D.C., Fox, P.M., Mackay, C.E., Filippini, N., Watkins, K.E., Toro, R., Laird, A.R., Beckmann, C.F., 2009. Correspondence of the brain's functional architecture during activation and rest. *Proc. Natl. Acad. Sci. USA* 106, 13040–13045.
- Smith, S.M., Jenkinson, M., Johansen-Berg, H., Rueckert, D., Nichols, T.E., Mackay, C.E., Watkins, K.E., Ciccarelli, O., Cader, M.Z., Matthews, P.M., Behrens, T.E.J., 2006. Tract-based spatial statistics: voxelwise analysis of multi-subject diffusion data. *NeuroImage* 31, 1487–1505.
- Smith, S.M., Jenkinson, M., Woolrich, M.W., Beckmann, C.F., Behrens, T.E.J., Johansen-Berg, H., Bannister, P.R., De Luca, M., Drobnjak, I., Flitney, D.E., Niazy, R.K., Saunders, J., Vickers, J., Zhang, Y., De Stefano, N., Brady, J.M., Matthews, P.M., 2004. Advances in functional and structural MR image analysis and implementation as FSL. *NeuroImage* 23 (Suppl. 1), S208–219.
- Smith, S.M., Nichols, T.E., 2009. Threshold-free cluster enhancement: addressing problems of smoothing, threshold dependence and localisation in cluster inference. *NeuroImage* 44, 83–98.
- Stoodley, C.J., Schmahmann, J.D., 2010. Evidence for topographic organization in the cerebellum of motor control versus cognitive and affective processing. *Cortex J. Devoted Study Nerv. Syst. Behav.* 46, 831–844.
- Stoodley, C.J., Valera, E.M., Schmahmann, J.D., 2012. Functional topography of the cerebellum for motor and cognitive tasks: an fMRI study. *NeuroImage* 59, 1560–1570.
- Strick, P.L., Dum, R.P., Fiez, J.A., 2009. Cerebellum and nonmotor function. *Annu. Rev. Neurosci.* 32, 413–434.
- Suzuki, L., Coulon, P., Sabel-Goedknegt, E.H., Ruigrok, T.J.H., 2012. Organization of cerebral projections to identified cerebellar zones in the posterior cerebellum of the rat. *J. Neurosci.* 32, 10854–10869.
- Tan, R.H., Devenney, E., Dobson-Stone, C., Kwok, J.B., Hodges, J.R., Kiernan, M.C., Halliday, G.M., Hornerger, M., 2014. Cerebellar integrity in the amyotrophic lateral sclerosis – frontotemporal dementia continuum. *PLoS One* 9.
- Tedeschi, G., Troisi, F., Tessitore, A., Corbo, D., Sagnelli, A., Paccone, A., D'Ambrosio, A., Piccirillo, G., Cirillo, M., Cirillo, S., Monsurrò, M.R., Esposito, F., 2012. Interaction between aging and neurodegeneration in amyotrophic lateral sclerosis. *Neurobiol. Aging* 33, 886–898.
- Thivard, L., Pradat, P.-F., Lehéricy, S., Lacomblez, L., Dormont, D., Chiras, J., Benali, H., Meininguer, V., 2007. Diffusion tensor imaging and voxel based morphometry study in amyotrophic lateral sclerosis: relationships with motor disability. *J. Neurol. Neurosurg. Psychiatry* 78, 889–892.
- Tona, F., De Giglio, L., Petsas, N., Sbardella, E., Prosperini, L., Upadhyay, N., Gianni, C., Pozzilli, C., Pantano, P., 2017. Role of cerebellar dentate functional connectivity in balance deficits in patients with multiple sclerosis. *Radiology* 287, 267–275.
- Troisi, F., Caiazzo, G., Corbo, D., Piccirillo, G., Cristillo, V., Femiano, C., Ferrantino, T., Cirillo, M., Monsurrò, M.R., Esposito, F., Tedeschi, G., 2015. Microstructural changes across different clinical milestones of disease in amyotrophic lateral sclerosis. *PLOS One* 10, e0119045.
- Turner, M.R., 2011. MRI as a frontrunner in the search for amyotrophic lateral sclerosis biomarkers? *Biomark Med.* 5, 79–81.
- Verstraete, E., van den Heuvel, M.P., Veldink, J.H., Blanck, N., Mandl, R.C., Hulshoff Pol, H.E., van den Berg, L.H., 2010. Motor network degeneration in amyotrophic lateral sclerosis: a structural and functional connectivity study. *PLoS One* 5, e13664.
- Zhou, C., Hu, X., Hu, J., Liang, M., Yin, X., Chen, L., Zhang, J., Wang, J., 2016. Altered brain network in amyotrophic lateral sclerosis: a resting graph theory-based network study at voxel-wise level. *Front. Neurosci.*
- Zhou, F., Gong, H., Li, F., Zhuang, Y., Zang, Y., Xu, R., Wang, Z., 2013. Altered motor network functional connectivity in amyotrophic lateral sclerosis: a resting-state functional magnetic resonance imaging study. *Neuroreport* 24, 657–662.